An event-based methodology to estimate emissions from upstream O&G sites

Mozhou Gao[1,3,4] (mozhou.gao@ucalgary.ca), Zahra Ashena[1,3] (zahra.bagheriashena@ucalgary.ca), Steve H.L. Liang[1,3] (liangs@ucalgary.ca), Sina Kiaei[1,3] (sina.kiaei@ucalgary.ca), and Sara Saeedi[1,2] (ssaeedi@ucalgary.ca)

[1]GeoSensorWeb Lab, Department of Geomatics Engineering, Schulich School of Engineering, University of Calgary, 2500 University Dr. NW, Calgary, AB, Canada

[2]Department of Electrical and Software Engineering, Schulich School of Engineering, University of Calgary, 2500 University Dr. NW, Calgary, AB, Canada

[3]SensorUp Inc, Calgary, AB, Canada

[4]Kuruktag Emissions Ltd, Coquitlam, BC, Canada

Email: mozhou.gao@ucalgary.ca

Abstract

Estimating annual site-level emissions in the oil and gas (O&G) sector is a key requirement for regulatory and voluntary initiatives worldwide. This study introduces an Emission Event Data Model (EEDM) that applies Allen's interval algebra and spatial proximity to group multi-scale emissions observation and O&G operational data into discrete events. The model classifies emissions events into three categories: resolved (known emission rate and duration), partially resolved (known emission rate but unknown or estimated duration), and unresolved (unknown emission rate and duration). To support the application of this data model, we developed a framework integrating numerical and simulation methods to calculate total emissions and associated uncertainties. The framework includes three Monte Carlo-based approaches to enhance emissions estimation: (1) estimating the duration of partially resolved events by incorporating null detects, leak production, and natural repair processes; (2) simulating emissions below the detection limits of deployed measurement technologies; and (3) estimating emissions from unresolved events by combining the probability of emission occurrences with best-fit emission rate and duration distributions. To demonstrate this framework, we estimated site-level emissions for a fictitious site using synthetic emission observations, including OGI inspection records, continuous monitoring systems data, aircraft flyovers, and O&G operational data. The proposed data model and methodologies have important implications for improving annual emissions reporting, reducing uncertainties, and supporting measurement-informed inventories, particularly under the Measuring, Monitoring, Reporting, and Verification (MMRV) framework.

Synopsis：This study addresses the fundamental data integration challenges in emissions estimation and well-suited for aligning with the MMRV framework.

Introduction

Reducing methane (CH_4) emissions from the oil and gas (O&G) sector is internationally recognized as one of the most cost-effective strategies for mitigating global warming [1]. This effort gained significant momentum following the launch of the Global Methane Pledge [2] at the 2021 United Nations Climate Change Conference (COP26), which set an ambitious goal of reducing methane emissions by 30% from 2020 levels by 2030. Since then, stakeholders worldwide have made substantial efforts to develop innovative measurement technologies and emissions estimation frameworks. Regulators, such as the U.S. Environmental Protection Agency (EPA) and the European Commission (EC), have further tightened regulatory requirements in recent years [3,4] to help achieve these reduction targets.

The Measuring, Monitoring, Reporting, and Verification (MMRV) framework is widely recognized as one of the most effective approaches for managing emissions in the oil and gas (O&G) sector and tracking annual emissions [5,6].

To date, MMRV or equivalent frameworks have primarily been adopted by voluntary initiatives such as the Oil and Gas Methane Partnership (OGMP) 2.0, the MiQ standard, and Veritas 2.0 [6–8]. Additionally, some regulatory initiatives, such as Air Quality Control Commission Regulation 7, Part B, implemented by the Colorado Department of Public Health and Environment (CDPHE), have also incorporated similar frameworks [9]. The key objectives of integrating MMRV into emissions reporting and management include reconciling emissions estimates from bottom-up (BU) and top-down (TD) approaches, creating a measurement-informed inventory (MII), and assessing overall carbon intensity across the supply chain.

Various technical challenges and the inherent characteristics of emissions hinder the effective implementation of MMRV by O&G operators. These challenges include the omission of super-emitters in conventional BU approaches, limited availability of measurement data, insufficient temporal and spatial coverage of remote O&G sites, undocumented operational activities, inaccuracies in emissions attribution, and the lack of unified measurement scales for emissions data [5,10–12].

To address these challenges and generate a more accurate MII, the scientific community has been actively developing hybrid approaches that integrate both BU and TD data. This includes exploring the potential of continuous monitoring systems (CMS), applying advanced statistical methods, and developing simulation approaches [13–18]. However, a comprehensive framework and standardized approach for assimilating emissions data from different measurement scales is still under development, particularly regarding the inclusion of emission duration. Such a framework is crucial for improving emissions estimation and reducing uncertainties.

This work introduces the first Emissions Event Data Model (EEDM) designed to spatially and temporally integrate multi-scale emissions measurements with O&G operational data. The model is developed based on the International Organization for Standardization (ISO) 19156:2023 and the Open Geospatial Consortium (OGC) 20-082r4 standards, and it integrates with the OGC Sensor Web Enablement suite [19–21]. Based on this data model, we classify emission events into three types and develop both numeric and simulation methodologies to resolve individual events, which are then combined to estimate total site-level emissions and their associated uncertainties. We believe the proposed data model and methodologies can be incorporated into the MMRV framework to achieve more accurate emissions estimation. To demonstrate the methodology and EEDM, we present two case studies using a fictitious site and synthetic emissions data.

Method and Materials

Emissions Event Data Model (EEDM)

Conventionally, methane emission data are modeled and managed for each emissions observation (EO). This process captures any form of detection, null-detection, or operational data indicating the presence or absence of CH_4 pollutants in the atmosphere, along with the timing (when) and location (where) of emissions occurred and the quantity (how much) emitted. This information helps attribute each emission observation to a specific physical source (e.g., equipment) and a cause (e.g., fugitive emissions, tank venting, etc.). However, emission observations are typically discrete in time and space, captured at different scales, and quantified using different algorithms. For example, snapshot emission observations, such as aircraft flyover measurements, provide a more accurate quantification of emissions from a site. In contrast, point-based CMS have lower detection limits and capture emission duration but only measure CH_4 at a fixed location, making them less accurate than aircraft flyovers in quantifying emissions.

To address the challenges, EEDM (Figure 1) was proposed based on the OGC standards, including ISO/OGC's Observations and Measurements 19156:2023/OGC 20-082r4 [19] and W3C/OGC Semantic Sensor Networks [21]. EEDM provides a consistent foundation aimed at enhancing the estimation of emissions duration and capturing their dynamic aspects, such as the lifecycle of leaks.
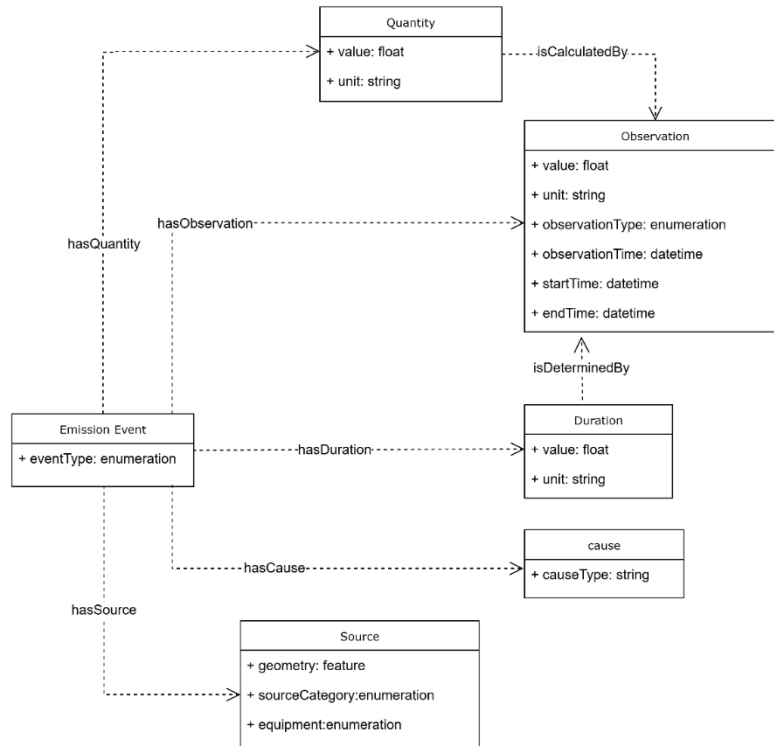
Quantity
+ value: float
+ unit: string

isCalculatedBy

Observation
+ value: float
+ unit: string
+ observationType: enumeration
+ observationTime: datetime
+ startTime: datetime
+ endTime: datetime

hasObservation

hasQuantity

isDeterminedBy

Emission Event
+ eventType: enumeration

hasDuration

Duration
+ value: float
+ unit: string

hasCause

cause
+ causeType: string

hasSource

Source
+ geometry: feature
+ sourceCategory:enumeration
+ equipment:enumeration

Figure 1. The entities and properties of the EEDM and their relationships. Formal definition can be found in S1 of the Supporting Information (SI).

Spatial and Temporal Correlation of Emissions Event (EE)

An emission event (EE) may consist of either a single observation or multiple observations capturing the same emission. To determine whether multiple observations can be grouped in both space and time, we apply spatial proximity [22] and Allen's interval algebra [23]. Spatial proximity assesses whether observations are geographically close or attributed to the same source (e.g., Compressor No. 1), while Allen's interval algebra (Table S1) determines the temporal relationships between observations. If two or more observations satisfy any of the other eleven relationships and are also spatially close (or attributed to the same equipment), they are more likely to observe the same emission event. More detail and formal definition of EEDM can be found in S1 of the Supporting Information (SI)

In addition to EO, an EE consists of four other primary components: source, cause, duration, and quantity. The source refers to any equipment or activity that emits methane, and EOs can be attributed to a specific physical source (e.g., Compressor No. 1), a source category (e.g., fugitive emissions, tank venting), or both (e.g., hydraulic fracturing from a gas well). The cause of an emission event ties to the results of a root cause analysis and is not limited to predefined categories. All observations within the same event should share a common cause. The duration of EE can be either directly measured using CMS (e.g., start and end times) or estimated through indirect

observations, such as the absence of emissions or null detection. Lastly, the quantity represents the total amount of methane emitted during the event.

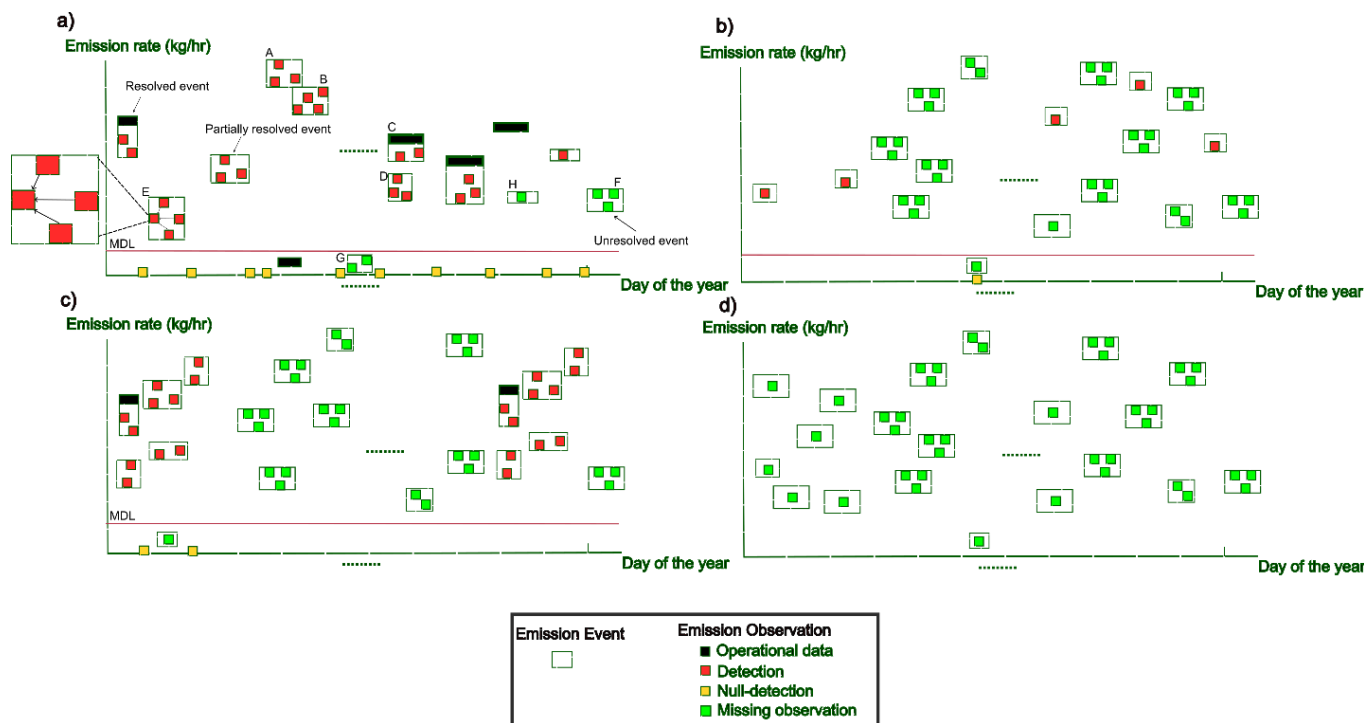Resolved Event, Partially Resolved Event, and Unresolved Event

Figure 1. Representation of resolved, partially resolved, and unresolved emission events at a site under four different monitoring scenarios throughout the year. Distinct colors, including operational data, detections, null-detections, and missing observations, indicate various observation types. Green dashed square boxes represent emission events. (a) A site with CMS measuring emissions 24 hours a day; (b) A site monitored through flyover surveys conducted every few months; (c) A site with a measurement campaign in which emissions are only measured during the campaign; and (d) A site without any monitoring.

We classify EE into three types (see Table S2): resolved events (REs), partially resolved events (PREs), and unresolved events (UEs). REs include EOs from data sources such as operational logs, which can be directly used to estimate duration, attribute sources, and perform root cause analysis. In contrast, PREs consist solely of EO from measurement technologies. They may require additional information to determine their duration and root cause, such as estimating duration using null detections from aircraft flyovers or routine leak detection and repair (LDAR) surveys that do not identify emissions. The unmeasured and undocumented emissions are classified as unresolved events (UEs), which can be classified into three types:

- **Type 1:** This occurs when emissions are present, but their rate falls below the minimum detection limit (MDL) of the deployed technology (e.g., event G in Figure 1a). This type of UE, also known as a false negative, represents an undetected emission event.

- **Type 2:** This happens when no measurement technology is deployed to detect the emission (e.g., event F in Figure 1a).

- **Type 3:** This occurs when a small fugitive emission coincides with a large operational EE (e.g., event H in Figure 1a) from the same equipment. Since the emission rates of both events cannot be separated, Type 3 UEs are typically omitted.

To ensure that each physical emission source (or equipment) has a unique event within each time period, we apply spatial proximity and Allen's interval algebra to merge events. For example, event A and event B can be merged if event A overlaps with event B. Similarly, event C and event D can be merged if event C contains event D, as shown in Figure 1a.

By following the structure of RE, PRE, and UE, the total annual emission of a given site (E_{total}) can be calculated as follows:

$$E_{Total} = \sum_{i_{RE}=1}^{N_{RE}} E_{RE_i} + \sum_{i_{PRE}=1}^{N_{PRE}} E_{PRE_i} + \sum_{i_{UE}=1}^{N_{UE}} E_{UE_i} \qquad\qquad Eq.1$$

where N_{RE}, N_{PRE} and N_{UE} indicates the number of resolved, partially resolved, and unresolved events, respectively. The E_{RE}, E_{PRE}, and E_{UE} represents total CH$_4$ emissions from each resolved, partially resolved, and unresolved event, respectively.

Based on how measurement technologies are deployed on-site, other scenarios of EEs include:

- **Instantaneous screening survey only**: If a site has only been surveyed using instantaneous measurement technologies, such as bi-monthly flyovers (Figure 1b). In that case, E_{RE} is zero, and total emissions will be calculated only by summing E_{PRE} and E_{UE}.
- **Measurement campaign only**: If a site has only been surveyed during an annual or bi-annual measurement campaign (Figure 1c), only limited numbers of REs and PREs are measured during the measurement campaign. Thus, E_{UE} must be simulated for periods that are outside the measurement campaign.
- **No Measurements:** If a site has no measurements at all (Figure 1d), both E_{PRE} and E_{RE} are zero, and E_{UE} must be simulated for the entire year.

Generic emissions estimation equation for EE

The total emissions (E) from an event can be calculated by the following:

$$E = Q \times D \qquad\qquad Eq.\ 2$$

where Q and D are the emission rate and duration of the event, respectively.

Resolved Event (RE)

For REs, the uncertainties associated with each event primarily arise from rate estimation uncertainty as durations are determined using operational data, which their uncertainty can be neglected. Therefore, the emission estimation of a RE (E_{RE}) with associated uncertainty (U_{E_RE}) can be expressed as follows:

$$E_{RE} = Q_{RE} \times D_{opt} \pm U_{Q\_RE} \times D_{opt} = Q_{RE} \times D_{opt} \pm U_{E\_RE} \qquad Eq.\ 3$$

where the emission rate (Q_{RE}) is obtained either from engineering calculations or quantified from measurement technology with the associated emission rate's quantification uncertainty (U_{Q_RE}). The duration (D_{opt}) is associated with operational data.

Partially Resolved Event (PRE)

Unlike REs, the uncertainty of PREs must account for both quantification and duration uncertainties. For PREs that include observations from CMS, start and end times are calculated based on measured CH_4 concentrations. However, studies have shown that the resulting durations can significantly differ from actual durations [23, 24]. Addressing this uncertainty requires time series analysis of in-situ wind direction and CH_4 concentration measurements, such as the Probabilistic Duration Model [23]. In contrast, the duration of PREs based solely on instantaneous observations is often estimated using rules or times derived from the preceding null-detects time (PNDT) and succeeding null-detects time (SNDT) [25]. As a result, these duration estimates may either overestimate or underestimate actual durations.

To improve duration accuracy for this type of PRE, we developed an event-based Monte Carlo simulation workflow that integrates the leak production rate (LPR) and null repair rate (NRR), both of which are implemented in established stochastic models such as LDAR-Sim and FEAST [27-29]. Figures S1 and S2 of the Supporting Information provide a detailed description of the time-bounded Monte Carlo simulation workflow. In the simulation, the PNDT and SNDT of PRE constrain the simulation's start and end times. The duration of the PRE is determined by sampling from binomial distributions based on the LPR and NRR. After 10^5 iterations, the median and the 2.5- and 97.5-percentiles of simulated durations are used to represent the final simulated duration and the associated duration uncertainty.

By integrating both the uncertainty from duration estimation and the uncertainty from quantification (U_{E_PRE}), the E_{PRE} of each PRE can be calculated by using the below equation:

$$E_{PRE} = Q_{PRE} \times D_{PRE} \pm U_{E\_PRE} \qquad Eq.4$$

where the D_{PRE} can be calculated or simulated as follows:

$$D_{PRE} = \begin{cases} T_{end} - T_{start}, & \text{if determined using CMS measurement} \\ \overline{D_{sim}}, & \text{if determined using null detect or rule} \end{cases} \qquad Eq.5$$

The error propagation equations [29] can be used to calculate the overall uncertainty of the PRE:

$$U_{E\_PRE} = \sqrt{\left(U_{Q_{PRE}}\right)^2 + (U_{D_{PRE}})^2} \qquad\qquad Eq.6$$

where $U_{D_{PRE}}$ can be calculated as follows:

$$U_{D_{PRE}} = \begin{cases} PDM(T_{end}, T_{start}, C_{CH4}), & \text{if determined using CMS measurement} \\ [D_{sim\_2.5\%}, D_{sim\_97.5\%}], & \text{if determined using nondetect or rule} \end{cases} \qquad Eq.7$$

Estimating emissions and uncertainty from UEs

We developed two distinct simulation approaches to estimate emissions from UEs at a given site. The first simulation integrates Johnson et al.'s [14] methodology into our EEDM framework by using a probability of detection (POD) equation and a stochastic process to identify UEs below the MDL of the deployed technologies. This approach is appropriate for sites with sufficient measurements (see S4 of SI).

The second simulation addresses scenarios where CMS is absent or instantaneous screening surveys that are infrequent. Rather than relying on POD, it simulates UEs based on the likelihood of emission event occurrence (see S5 of SI). This method ensures that simulated UEs are based on site-specific characteristics by using data from the same site when sufficient REs and PREs are available for the given site or by deriving probabilities from sites with the same emissions characteristics when they are not. The rate and duration of each sampled UE are also sampled from distributions constructed using measured rates and durations of REs and PREs. Sampling duration can effectively address the intermittency of UEs [31]. Figures S2 and S3 illustrate the workflow of these two simulation approaches. Since both simulations are based on the Monte Carlo approach, 10^5 iterations are required, and the median, along with the 2.5th and 97.5th percentiles of the simulation results, is calculated to represent the simulated emissions from UEs and their associated uncertainty.

Estimating emissions and uncertainties across all EEs

By integrating the simulated emissions from UEs ($\bar{E}_{UE\_sim}$), *Eq. 1* to *Eq.4* can be rewritten as

$$E_{Total} = \sum_{i_{RE}=1}^{N_{RE}} Q_{RE_i} \times D_{opt_i} + \sum_{i_{PRE}=1}^{N_{PRE}} Q_{PRE_i} \times D_{PRE_i} + \bar{E}_{UE\_sim} \qquad Eq.8$$

and the total uncertainty associated with E_{Total} can be calculated as follows:

$$U_{E\_total} = \frac{\sqrt{(U_{E\_REs} \times E_{REs})^2 + (U_{E\_PREs} \times E_{PREs})^2 + (U_{E\_REs} \times E_{UEs})^2}}{|E_{REs} + E_{PREs} + E_{UEs}|} \qquad Eq.9$$

The detailed derivation of the equation can be found in S2 of SI.

Case Studies

To demonstrate our methodologies, we developed two distinct case studies that estimate total emissions from a fictitious site with ten pieces of equipment over the period from January 1, 2024, to April 30, 2024. The first case study utilizes 146 simulated emission observations—including 89 CMS measurements, four flyover survey records (one of which did not detect any plume), four OGI inspection records (two of which did not find any leaks), and 49 venting data points. Due to the sufficient number of observations, emissions from UEs are simulated using a POD-based approach. The second case study extrapolates emissions based on the probability of EE occurrence using only 36 CMS observations collected during a single month. More details of synthetic EOs can be found in S6 of the Supporting Information.
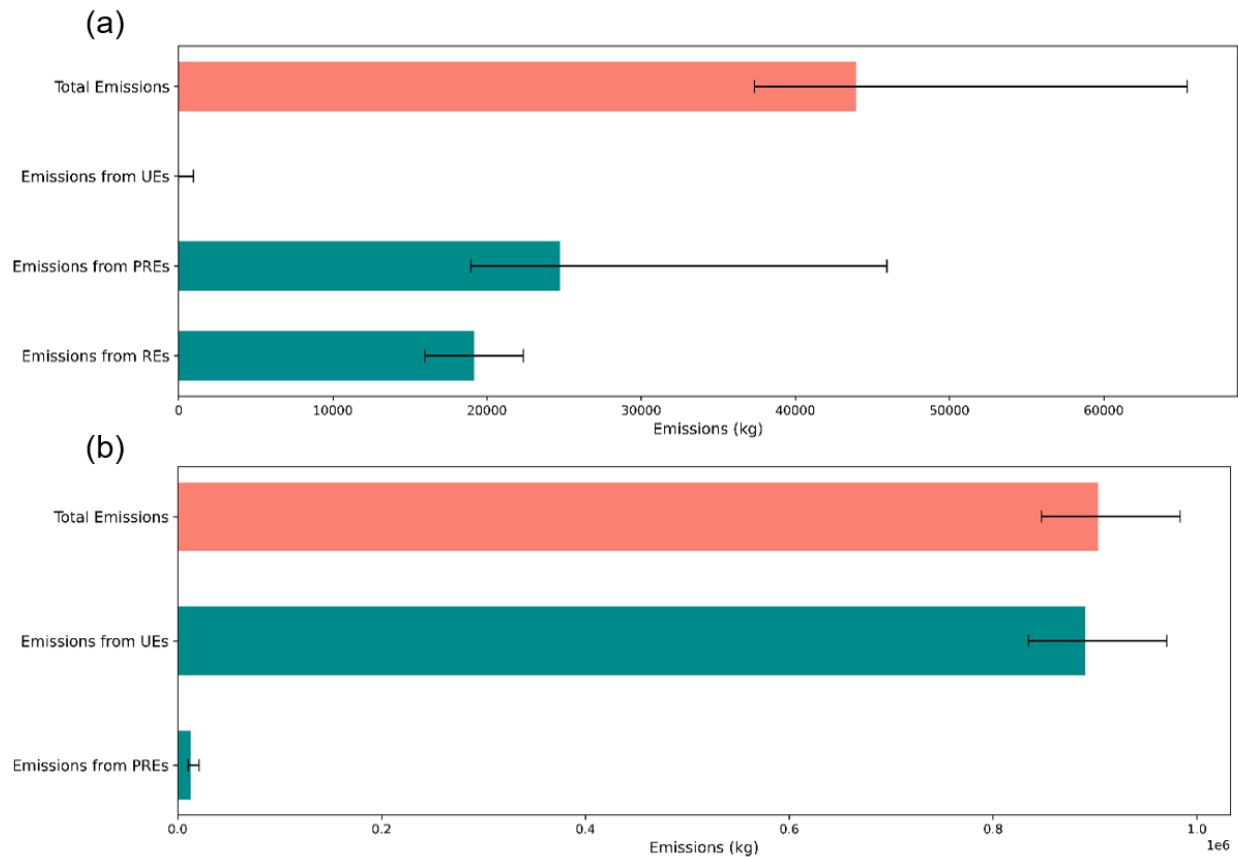
Results

Figure 2. The bar chart shows the total site-level emission estimates and breakdown of REs, PREs, and UEs emissions from (a) case study No.1 and (b) case study No.2.

Figure 2a illustrates the total emissions and their associated uncertainties. After merging the events, only one PRE had its duration estimated using null detections. The resulting distribution of simulated durations was right-skewed, with a median duration of 116.75 hours and a 95% confidence interval (CI) of [4.75, 606.75]. The total emissions over four months are 43922.09 kg,

with 95% CI [37336.08, 65408.83]. The breakdown of emissions from REs and PREs are 19167.56 kg (95% CI [15959.26, 22375.86]) and 24719.31 kg (95% CI [18967.67, 45945.20]).

Figure 2b represents the calculation results for total emissions from PREs, which were 12,752.90 kg, with a 95% CI [10,318.35, 21,225.40]. After adding 890,185.12 kg of simulated emissions from UEs using the second simulation, the total four-month emissions for the fictitious site were 902,938.02 kg, with a 95% CI [847,296.82, 983,393.09].

Calculations for both case studies were performed in Python, and more detailed descriptions of the synthetic observations can be found in S7 of the SI.

Implications

We introduce a new framework integrating multi-scale measurements and O&G operational data to construct emission events. Adopting ISO & OGC standards ensures that emission events are compatible across diverse technologies. This integration enhances source attribution and root cause analysis by combining sensor data with operational records.

Differentiating between REs and PREs improves uncertainty assessments. Past studies have found that most simulated events are short-duration [32]. Partitioning emissions from intermittent sources to multiple short-duration events can significantly reduce the overall uncertainties in emissions estimation.

In Case Study 2, distributions and probabilities are calculated for each equipment unit. These metrics can also be derived for individual activities or source categories to align with reporting frameworks, such as OGMP 2.0.

Beyond site-level emission estimates, EEDM is also suited for responding to the Super-Emitter Program under US EPA regulations [3, 32]. EEDM can more effectively track the source and results from root cause analysis. The start and end times can be more clearly defined by grouping a super-emitter observation (e.g., flyover) and OGI follow-up into a single event.

Our model supports the creation of an MII and is compatible with known voluntary initiative frameworks, such as Best-measured vs. Best-calculated from Veritas 2.0 and OGMP 2.0 Level 4 and 5 emissions reporting. REs and PREs can be grouped by source to classify events for each source (one class of EEDM). For instance, an MII-based emission factor and its associated uncertainty for flaring can be calculated by dividing the total emissions by the total number of flaring events. The remaining gap in the framework is the lack of a QA/QC process to validate input EOs. Future research will aim to demonstrate EEDM and the presented methodologies using real emissions measurements and operational data.

Code and Data availability

The analysis was programmed in Python with standard packages. The scripts will be provided upon request. The data required to perform simulations are also included in the Supplementary Information and GitHub repository. The results can be reproduced by employing the equations, explanations, and parameters provided in the main text. Additional code and data will be made available upon request.

Disclosure statement

No potential conflict of interest was reported by the author (s).

Author contributions

M.G and S. L designed the research. M.G. directed and performed the analyses. M.G. and Z. A. wrote the paper. M.G., S.L., Z.A., S.S. and S. K. edited the paper.

References

1. International Energy Agency. *Global Methane Tracker 2023*; IEA: 2023. Available at: https://www.iea.org/reports/global-methane-tracker-2023.
2. United Nations Framework Convention on Climate Change. *Global Methane Pledge*; UNFCCC: 2021. Available at: https://www.globalmethanepledge.org.
3. U.S. Environmental Protection Agency. *Revisions to GHGRP Subpart W: Petroleum and Natural Gas Systems*; U.S. EPA: 2023. Available at: https://www.epa.gov/inflation-reduction-act/revisions-ghgrp-subpart-w-petroleum-and-natural-gas-systems.
4. European Commission. *New EU Methane Regulation to Reduce Harmful Emissions from Fossil Fuels in Europe and Abroad*; European Commission: 2024. Available at: https://energy.ec.europa.eu/news/new-eu-methane-regulation-reduce-harmful-emissions-fossil-fuels-europe-and-abroad-2024-05-27_en.
5. Allen, D.; Revikumar, A.; Tullos, E. Scientific Challenges of Monitoring, Measuring, Reporting, and Verifying Greenhouse Gas Emissions from Natural Gas Systems. *ACS Sustainable Resour. Manage.* **2023**, *1* (1), 10–12. https://doi.org/10.1021/acssusresmgt.3c00132.
6. United Nations Environment Programme. *The Oil & Gas Methane Partnership 2.0 (OGMP 2.0)*; UNEP: 2020. Available at: https://ogmpartnership.com/.
7. MiQ. *The MiQ Standard: A Framework for Methane Emissions Assessment*; MiQ: 2024. Available at: https://miq.org/the-technical-standard/.
8. GTI Energy. *Veritas: Ensuring Accurate Methane Emissions Measurements in the Oil and Gas Industry*; GTI Energy: 2024. Available at: https://www.gti.energy/veritas/.

9. Colorado Department of Public Health & Environment. *Air Quality Control Commission Regulation Number 7*; CDPHE: 2024. Available at: https://cdphe.colorado.gov/aqcc-regulations.

10. Vaughn, T. L.; et al. Temporal Variability Largely Explains Top-Down/Bottom-Up Difference in Methane Emission Estimates from a Natural Gas Production Region. *Proc. Natl. Acad. Sci. U.S.A.* **2018**, *115*, 11712–11717. https://doi.org/10.1073/pnas.1805687115.

11. Brandt, A. R.; Heath, G. A.; Cooley, D. Methane Leaks from Natural Gas Systems Follow Extreme Distributions. *Environ. Sci. Technol.* **2016**, *50*, 12512–12520. https://doi.org/10.1021/acs.est.6b04303.

12. Scarpelli, T. R.; et al. Updated Global Fuel Exploitation Inventory (GFEI) for Methane Emissions from the Oil, Gas, and Coal Sectors: Evaluation with Inversions of Atmospheric Methane Observations. *Atmos. Chem. Phys.* **2022**, *22*, 3235–3249. https://doi.org/10.5194/acp-22-3235-2022.

13. Rutherford, J. S.; et al. Closing the Methane Gap in U.S. Oil and Natural Gas Production Emissions Inventories. *Nat. Commun.* **2021**, *12*. https://doi.org/10.1038/s41467-021-25017-4.

14. Johnson, M. R.; Conrad, B. M.; Tyner, D. R. Creating Measurement-Based Oil and Gas Sector Methane Inventories Using Source-Resolved Aerial Surveys. *Commun. Earth Environ.* **2023**, *4*. https://doi.org/10.1038/s43247-023-00769-7.

15. Riddick, S. N.; et al. Estimating Total Methane Emissions from the Denver-Julesburg Basin Using Bottom-Up Approaches. *Gases* **2024**, *4*, 236–252. https://doi.org/10.3390/gases4030014.

16. Wang, J. L.; Daniels, W. S.; Hammerling, D. M.; Harrison, M.; Burmaster, K.; George, F. C.; Ravikumar, A. P. Multiscale Methane Measurements at Oil and Gas Facilities Reveal Necessary Frameworks for Improved Emissions Accounting. *Environ. Sci. Technol.* **2022**, *56*, 14743–14752. https://doi.org/10.1021/acs.est.2c06211.

17. MacKay, K.; et al. A Comprehensive Integration and Synthesis of Methane Emissions from Canada's Oil and Gas Value Chain. *Environ. Sci. Technol.* **2024**, *58*, 14203–14213. https://doi.org/10.1021/acs.est.4c03651.

18. Daniels, W. S.; et al. Toward Multiscale Measurement-Informed Methane Inventories: Reconciling Bottom-Up Site-Level Inventories with Top-Down Measurements Using Continuous Monitoring Systems. *Environ. Sci. Technol.* **2023**, *57*, 11823–11833. https://doi.org/10.1021/acs.est.3c01121.

19. International Organization for Standardization. *ISO 19156:2023 Geographic Information— Observations, Measurements, and Samples*; ISO: 2023. Available at: https://www.iso.org/standard/82463.html#lifecycle.

20. Reed, C.; Botts, M.; Percivall, G.; Davidson, J. *OGC® Sensor Web Enablement: Overview and High-Level Architecture*; Open Geospatial Consortium: 2013. Available at: https://docs.ogc.org/wp/07-165r1/.

21. World Wide Web Consortium. *Semantic Sensor Network Ontology*; W3C: 2017. Available at: https://www.w3.org/TR/2017/REC-vocab-ssn-20171019/.

22. Anselin, L. Local Indicators of Spatial Association—LISA. *Geogr. Anal.* **1995**, *27*, 93–115. https://doi.org/10.1111/j.1538-4632.1995.tb00338.x.

23. Allen, J. F. Maintaining Knowledge about Temporal Intervals. *Commun. ACM* **1983**, *26*, 832–843. https://doi.org/10.1145/182.358434.

24. Daniels, W. S.; Jia, M.; Hammerling, D. M. Estimating Methane Emission Durations Using Continuous Monitoring Systems. *Environ. Sci. Technol. Lett.* **2024**, *11*, 1187–1192. https://doi.org/10.1021/acs.estlett.4c00687.

25. Bell, C.; et al. Performance of Continuous Emission Monitoring Solutions under a Single-Blind Controlled Testing Protocol. *Environ. Sci. Technol.* **2023**, *57*, 5794–5805. https://doi.org/10.1021/acs.est.2c09235.

26. Government of Canada. *Regulations Respecting Reduction in the Release of Methane and Certain Volatile Organic Compounds (Upstream Oil and Gas Sector) (SOR/2018-66)*; Canada Gazette: 2018. Available at: https://gazette.gc.ca/rp-pr/p2/2018/2018-04-26/html/sor-dors66-eng.html.

27. Fox, T. A.; Gao, M.; Barchyn, T. E.; Jamin, Y. L.; Hugenholtz, C. H. An Agent-Based Model for Estimating Emissions Reduction Equivalence among Leak Detection and Repair Programs. *J. Clean. Prod.* **2021**, *282*, 125237. https://doi.org/10.1016/j.jclepro.2020.125237.

28. Kemp, C. E.; Ravikumar, A. P.; Brandt, A. R. Comparing Natural Gas Leakage Detection Technologies Using an Open-Source "Virtual Gas Field" Simulator. *Environ. Sci. Technol.* **2016**, *50*, 4546–4553. https://doi.org/10.1021/acs.est.5b06068.

29. Kemp, C. E.; Ravikumar, A. P. *Fugitive Emissions Abatement Simulation Toolkit User Guide – FEAST v3.1 Guide & Technical Documentation*; FEAST: 2021. Available at: https://github.com/FEAST-SEDLab/FEAST_PtE/blob/FEAST_3.1/FEAST%203.1%20User%20Guide.pdf.

30. Intergovernmental Panel on Climate Change. *2006 IPCC Guidelines for National Greenhouse Gas Inventories: Volume 1. General Guidance and Reporting*; National Greenhouse Gas Inventories Programme: 2006; Hayama, Japan: IGES.

31. Wang, J. L.; Daniels, W. S.; Hammerling, D. M.; Harrison, M.; Burmaster, K.; George, F. C.; Ravikumar, A. P. Multiscale Methane Measurements at Oil and Gas Facilities Reveal Necessary Frameworks for Improved Emissions Accounting. *Environ. Sci. Technol.* **2022**, *56*, 14743–14752. https://doi.org/10.1021/acs.est.2c06211.

32. U.S. Environmental Protection Agency. *Standards of Performance for Crude Oil and Natural Gas Facilities for Which Construction, Modification, or Reconstruction Commenced after November 15, 2021 (40 C.F.R. § 60 Subpart OOOOb)*; U.S. EPA: 2023. Available at: https://www.ecfr.gov/current/title-40/chapter-I/subchapter-C/part-60/subpart-OOOOb.

Supporting Information for:

An event-based methodology to estimate emissions from upstream O&G sites

Mozhou Gao[1,3,4], Zahra Ashena[1,3], Steve H.L. Liang[1,3], Sina Kiaei[1,3], and Sara Saeedi[1,2]

[1]GeoSensorWeb Lab, Department of Geomatics Engineering, Schulich School of Engineering, University of Calgary, 2500 University Dr. NW, Calgary, AB, Canada

[2]Department of Electrical and Software Engineering, Schulich School of Engineering, University of Calgary, 2500 University Dr. NW, Calgary, AB, Canada

[3]SensorUp Inc, Calgary, AB, Canada

[4]Kuruktag Emissions Ltd, Coquitlam, BC, Canada

Email: mozhou.gao@ucalgary.ca

Table of Contents

S1. Emissions event data model (EEDM) and Allen's time algebra

The UML definition of the emissions event data model (EEDM) can be expressed as follows:

```
class EmissionsEvent {
    - eventType: enumeration
    - hasDuration: Duration
    - hasCause: Cause
    - hasSource: Source
    - hasQuantity: Quantity
    - hasObservation: Observation[*]
}

class Duration {
    + value: float
    + unit: string
}

class Cause {
    + causeType: string
}

class Source {
    + geometry: feature
    + sourceCategory: enumeration
    + equipment: enumeration
}

class Quantity {
    + value: float
    + unit: string
    - isCalculatedBy: Observation
    - isDeterminedBy: ObservationF
}

class Observation {
    + value: float
    + unit: string
    + observationType: enumeration
    + observationTime: datetime
    + startTime: datetime
    + endTime: datetime
}

class EventGrouping {
    - spatialProximity: boolean
    - temporalRelationship: enumeration
    - groups: EmissionsEvent[*]
}
```

Where *Obervation[*]* in EE allows multiple emissions observations (EOs) to be associated with a single EE. *EventGrouping* class is not included in the Figure 1 of main paper. It represents the logic of grouping EOs using spatial proximity and Allen's interval algebra. The *groups* tracks merged emission events.

To group EOs into a single EE or merge multiple EEs into one EE, the model uses spatial proximity to indicate if observations are geographically close or directly/indirectly attributed to the same physical emission sources (equipment). The *temporalRelationship* indicates the temporal relations between EOs or EEs based on Allen's Interval Algebra [1].

Table S1: Illustration of Allen's interval algebra logic between two-time intervals.

Relation	Illustration	
T1 precedes T2	T1	
T2 precededBy T1	T2	
T1 meets T2	T1	
T2 metBy T1	T2	
T1 overlaps T2	T1	
T2 overlappedBy T1	T2	
T1 starts T2	T1	
T2 startedBy T1	T2	
T1 during T2	T1	
T2 contains T1	T2	
T1 finishes T2	T1	
T2 finishedBy T1	T2	
T1 equals T2	T1	
	T2	

As illustrated in Table S1, thirteen fundamental temporal relationships are defined: *precedes, preceded by, meets, met by, overlaps, overlapped by, contains, during, starts, started by, finishes, finished by,* and *equals* [1]. Except for *precedes* and *preceded by*, if two or more EOs or EEs satisfy any of the other eleven relationships and are also spatially close (or attributed to the same equipment), they are more likely to originate from the same emission within the same emission event. For example, we can conclude that the CMS alarm and VFB can be correlated as the same event, when a CMS alarm indicating emissions from Compressor A between 2024-07-05T09:00:00 and 2024-07-05T11:00:00 *contains* Compressor rod packing venting reported for Compressor A from 2024-07-05T10:20:00 to 2024-07-05T10:50:00.

The EEDM uses a network of nodes and edges to identify temporal rules based on relationships between emission observations within the same event. Each observation is a node within an event, while edges represent the spatiotemporal correlations between them. The observation with the earliest timestamp is defined as the parent, and all other observations are considered child observations (see event E in Figure 1a). When two events merge, child and parent observations are

redefined accordingly. The parent observation plays a crucial role in PREs that contain only instantaneous measurement observations, particularly when duration must be inferred from preceding and succeeding null detections.

It is important to highlight that *precedes* and *precededBy* are specifically applied to intermittent emission events that have stopped and started again. In EEDM, we treat intermittent events as separate events.

For this study, we classify emission events into three types: resolved events (REs), partially resolved events (PREs), and unresolved event (UEs). Their definitions can be found in Table S2.

Table S2: Three categories of emission event types.

Emission Event Type	Definition	Duration Determination	Total Emissions from Events	Uncertainty
Resolved Event (RE)	Events with durations determined using operational data/log	Extracted from operational data/log	Calculated	Only quantification uncertainty is considered
Partially Resolved Event (PRE)	Events with duration that are either measured by remote sensing technologies or estimated using null-detection and rules	Simulated using proceeding and succeeding null-detection times	Calculated	Quantification uncertainty and duration estimation uncertainty
Unresolved Event (UE)	Events that are missing from annual emissions data	Simulated	(1) Simulate emissions that are not detected using POD checks (2) Simulate emissions by random sample RE and PRE	Estimated in the simulations

Based on above definitions, we can define the three types of EE mathematically based on following expressions.

Let:

E be the set of all emission events.

RE, PRE and UE be the subsets of E corresponding to Resolved Events, Partially Resolved Events, and Unresolved Events, respectively.

EO_m be the set of emissions observations from measurement technologies.

EO_o be the set of emissions observations from operational logs.

N be the set of null-detection data (including from screening survey or LDAR inspection).

U be the set of emissions data that are not captured by any emissions observations.

Then we can define each emission event type as:

For resolved events (REs):

$$RE = \{e \in E \mid e \text{ has at least one observation from } EO_o\}$$

For partially resolved events (PREs):

$$PRE = \{e \in E \mid e \text{ has at least one observation from } EO_m \text{ but lacks } EO_o\}$$

For unresolved event (UEs):

$$UE = \{e \in E \mid e \notin RE \cup PRE\} = \{e \in E \mid e \text{ has no observation from } EO_m \text{ or } EO_o\}$$

To ensure that every EE falls into exactly one category:

$E = RE \cup PRE \cup UE,$

$RE \cup PRE = \emptyset,$

$RE \cup UE = \emptyset,$

$PRE \cup UE = \emptyset,$

S2. Derivation of equations associated with REs, PREs, and UEs

By following the structure of RE, PRE, and UE, the total annual emission of a given site (E_{total}) can be calculated by following *Eq.1*.

$$E_{Total} = \sum_{i_{RE}=1}^{N_{RE}} E_{RE_i} + \sum_{i_{PRE}=1}^{N_{PRE}} E_{PRE_i} + \sum_{i_{UE}=1}^{N_{UE}} E_{UE_i} \qquad\qquad Eq.1$$

where N_{RE}, N_{PRE}, and N_{UE} indicate the number of resolved events, partially resolved events, and unresolved events, respectively. The E_{RE}, E_{PRE}, and E_{UE} represent total CH_4 emissions from each resolved, partially resolved, and unresolved event, respectively.

The generic equation of calculating total emissions (E) of an event can be described as follows:

$$E = Q \times D \qquad\qquad Eq.\ 2$$

where, Q and D are emission rate, and duration of the event, respectively.

For REs, the uncertainties associated with emissions estimation of each event primarily arise from quantification. Since the operational data usually includes more accurate start and end times of a

venting event. The duration uncertainty is negligible. Technology vendors or survey providers usually include quantification uncertainty alongside the reported emission rate. For example, the quantification uncertainty of the Kairos/Insight M aircraft system is found to be approximately ±40% [2]. By incorporating the quantification uncertainty (U_{Q_RE}), the emission estimation of a RE (E_{RE}) can be expressed as follows:

$$E_{RE} = (Q_{RE} \pm U_{Q_{RE}}) \times D_{opt} = Q_{RE} \times D_{opt} \pm U_{Q\_RE} \times D_{opt} \qquad Eq.\ 3$$

where Q_{RE} is the rate, either obtained from engineering calculation or quantified from measurement technology, and D_{opt} is the duration associated with operational data. Therefore, the uncertainty of the RE (U_{E_RE}) can be calculated by multiplying the quantification uncertainty by the duration. *Eq. 3* can also be rewritten as follows:

$$E_{RE} = Q_{RE} \times D_{opt} \pm U_{E\_RE} \qquad Eq.\ 4$$

It should be noted that some engineering equations directly calculate the E_{RE}. In such cases, the uncertainty should be determined based on the equation used in the calculation.

For PREs, the uncertainties include both quantification error and duration estimation error. After integrating both, the E_{PRE} of each PRE can be calculated by using the below equation:

$$E_{PRE} = Q_{PRE} \times D_{PRE} \pm U_{E\_PRE} \qquad Eq.5$$

where the D_{PRE} can be calculated or simulated (see S3). The equation of estimating D_{PRE} can be expressed as follows:

$$D_{PRE} = \begin{cases} T_{end} - T_{start}, & \textit{if determined using CMS measurement} \\ \overline{D_{sim}}, & \textit{if determined using nondetect or rule} \end{cases} \qquad Eq.6$$

U_{E_PRE} represents uncertainties associated with the emissions estimated for each PRE. It consists of both quantification uncertainty ($U_{Q_{PRE}}$) and duration estimation uncertainty ($U_{D_{PRE}}$). Based on *Eq.7*, $U_{D_{PRE}}$ can be calculated as follows:

$$U_{D_{PRE}} = \begin{cases} PDM(T_{end}, T_{start}, C_{CH4}), & \textit{if determined using CMS measurement [3]} \\ [D_{sim\_2.5\%}, D_{sim\_97.5\%}], & \textit{if determined using nondetect or rule} \end{cases} \qquad Eq.7$$

To combine both uncertainties from quantification and duration estimations, we apply the error propagation equations described by IPCC [4,5].

$$U_{E\_PRE} = \sqrt{\left(U_{Q_{PRE}}\right)^2 + (U_{D_{PRE}})^2} \qquad Eq.8$$

The *Eq.8* assumes that duration estimation uncertainty and quantification uncertainty are uncorrelated. However, this assumption may not always be valid. For instance, in a PRE with a CMS measurement, the emission rate and duration are both measured or quantified by the same

sensor, introducing potential dependencies between the two uncertainties. While this correlation is important, a detailed investigation is beyond the scope of this study.

The total emissions from UEs ($\bar{E}_{UE\_sim}$) are entirely simulated (See S4 and S5). To combine emissions from all three event types, *Eq.1* can be rewritten as:

$$E_{Total} = \sum_{i_{RE}=1}^{N_{RE}} Q_{RE_i} \times D_{opt_i} + \sum_{i_{PRE}=1}^{N_{PRE}} Q_{PRE_i} \times D_{PRE_i} + \bar{E}_{UE\_sim} \qquad \textit{Eq. 9}$$

By following the uncertainty equation suggested by IPCC [4,5], the uncertainty (U_{E_RES}) associated with REs can be expressed as follows:

$$U_{E\_RES} = \frac{\sqrt{(U_{E\_RE_1} \times E_{RE_1})^2 + (U_{E\_RE_2} \times E_{RE_2})^2 + \ldots + (U_{E\_RE_{N_{RE}}} \times E_{RE_{N_{RE}}})^2}}{\left| E_{\_RE_1} + E_{RE_2} + \cdots + E_{RE_{N_{RE}}} \right|} \qquad \textit{Eq.10}$$

where U_{E_RE} is calculated in *Eq.3*.

For the uncertainty of PREs:

$$U_{E\_PRES} = \frac{\sqrt{(U_{E\_PRE_1} \times E_{PRE_1})^2 + (U_{E\_PRE_2} \times E_{PRE_2})^2 + \ldots + (U_{E\_PRE_{N_{PRE}}} \times E_{PRE_{N_{PRE}}})^2}}{\left| E_{PRE_1} + E_{PRE_2} + \cdots + E_{PRE_{N_{RE}}} \right|} \qquad \textit{Eq.11}$$

where U_{E_PRE} is calculated in *Eq.8*.

By combining *Eq 9-11*, the total uncertainty associated with E_{Total} can be calculated as follows:

$$U_{E\_total} = \frac{\sqrt{(U_{E\_RES} \times E_{RES})^2 + (U_{E\_PRES} \times E_{PRES})^2 + (U_{E\_RES} \times E_{UES})^2}}{|E_{RES} + E_{PRES} + E_{UES}|} \qquad \textit{Eq.12}$$

S3. Duration simulation
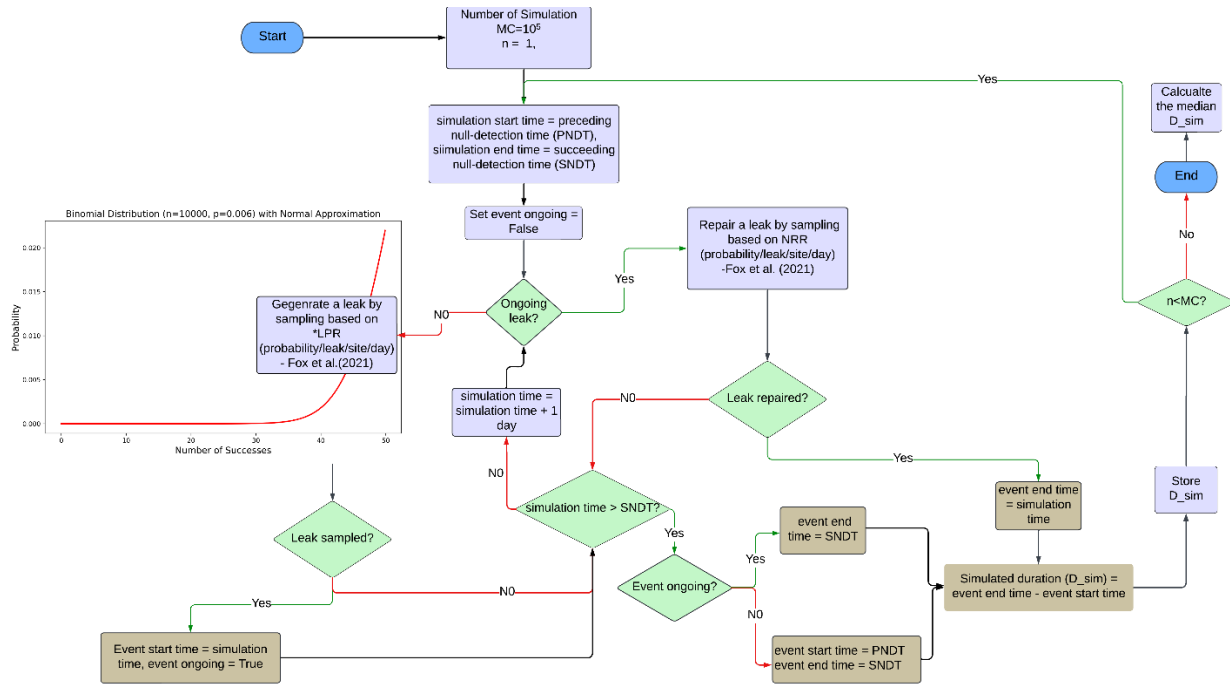
Figure S1. The Monte Carlo simulation workflow simulates the duration of a PRE based on the preceding null-detection and succeeding null-detection of the event. In the simulation, the units of LPR and NRR are per site per day. Here, we present an example binomial distribution with a probability of 0.006 to sample leaks across 10^5 iterations. *If LPR and NRR are calculated by equipment or component, the leak sampling and repairing processes iterate through each equipment or component based on equipment or component counts until all are checked.

For each PRE, a Monte Carlo simulation ($M = 10^5$ iterations) is performed to simulate the duration to ensure the stationary distribution of results. The start and end times of the simulation were bounded by the preceding null-detection time (PNDT) and succeeding null-detection time (SNDT), respectively. Each simulation iteration initializes the emission event as "not occurring." To determine the start time of the emission event, the simulation randomly samples from a binomial distribution based on an emission probability calculated using the LPR equation (Fox et al., 2021). If an emission is sampled, the timestamp of the simulation becomes the start time of the emission event, the simulation updates the status of event as ongoing, and the simulation proceeds to the next day. Otherwise, the simulation directly proceeds to the next day and repeats the sampling process. Once an emission event is ongoing, a second binomial distribution, based on a probability calculated using the NRR equation [6], is used to perform daily random sampling to determine event cessation. If the event is stopped, the simulation timestamp is saved as the simulated end time of the event; if not, the process continues to the next day until either the timestamp exceeds the SNDT, or an end time has been successfully determined. At the end of each simulation run, the simulated end time is set to the SNDT if the emission event remains ongoing. If no emission event occurred during the simulation, both the simulated start and end times are set to the PNDT and

SNDT, respectively. The simulated duration is then calculated as the difference between the simulated end and start times. After 10^5 iterations, the mean ($\overline{D_{sim}}$) and 2 times standard deviation of the differences between simulated and estimated durations are calculated to represent the uncertainty in duration and the uncertainty from random sampling under the 95% confidence interval. If simulation results are non-normally distributed, we use median and 2.5- ($D_{sim\_2.5\%}$) and 97.5-percentiles ($D_{sim\_97.5\%}$) to represent simulated duration and uncertainty [7].

S4. Simulating Emissions from UEs using probability of detection (POD)
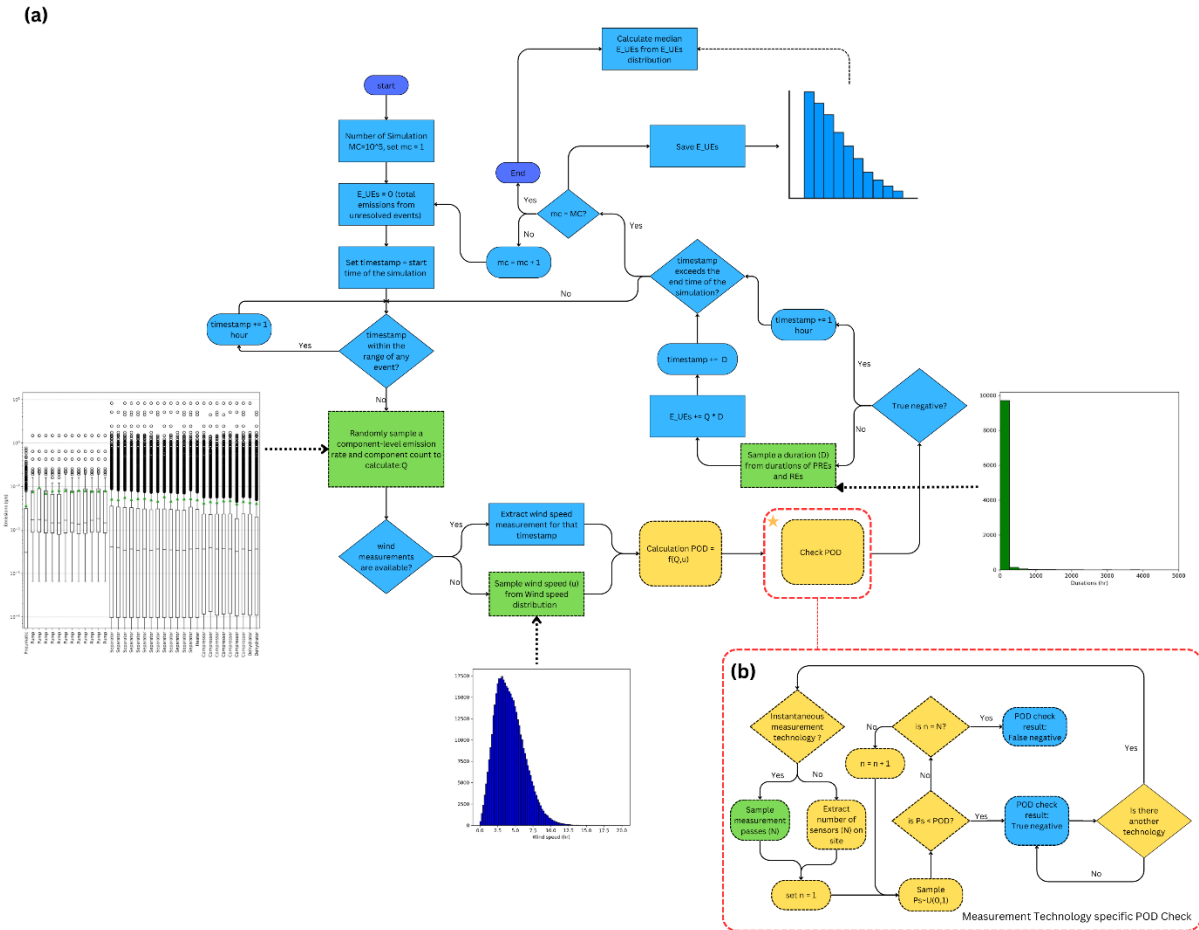
Figure S2. Monte Carlo simulation workflow to estimate total emissions from unresolved events for a given site that is monitored by flyover and CMS. This workflow specifically illustrates the scenario where emissions are measured by one type of aircraft flyover and one CMS; more probability of detection (POD) checks are required if other types of technology are also deployed for emission monitoring. [a]Component-level emissions distributions should be derived from real measurements [8]. [b]Different aircraft systems require different equations to calculate POD based on different parameters. For instance, Conrad et al. [9] provided POD equations for three different aircraft systems. Here, the flowchart only assumes the POD is affected by wind speed. [c]Similarly, Bell et al. [10] derived POD equations for multiple CMSs, which are also dependent on wind speed.

They are applicable in CMS POD checks as well. [d]The duration distributions are based on empirical data from partially resolved events (PREs) of the site or sites with similar characteristics.

As illustrated in Figure S2, the simulation workflow begins by initializing the simulation time to the start of the reconciliation period (usually the first day of the year for the annual reconciliation) and setting possible emissions from UEs (E_{UE_sim}) to 0. At each hourly timestep, the simulation checks if the current timestamp falls within the range of any emission event (both RE and PRE). If the timestamp exceeds the simulation range (e.g., the last day of the year), the simulation proceeds to the next iteration. If no emission event occurs in a given timestamp, a component-scale emission rate and component counts are sampled from either the inventory or database containing component-scale measurements to obtain an equipment-scale emission rate. Wind speed and flight passes for each flyover survey at the site location are also randomly sampled.

In Figure S2, we are using a site measured by both flyover and CMS as an example. The simulation determines the false negative and identifies if any measurement technology fails to detect an emission independently. Probability of detection (POD)s are calculated using the sampled emission rate and wind speed. Each calculated PODs are then compared to a randomly generated probability (ξ) between 0 and 1. If the POD exceeds ξ, it indicates a false negative (i.e., if the sampled emission occurred in the real world, it would not be detected). If the POD is smaller than ξ, it indicates a true negative (i.e., if the sampled emission occurred in the real world, it would be detected). This comparison is done for each flyover path and each sensor installed on the site. If either the flyover or CMS POD check returns false negative, the sampled emission rate is multiplied by a sampled duration (t_u) to consolidate a UE. Then, the resulted emissions are added to the cumulative E_{UE_sim}. The sampled duration is also added to the time step in the simulation. If POD checks from flyover and CMS both return true negative, meaning no emissions occurred at the time step, the simulation proceeds to the next hour. This process is repeated until the timestamp exceeds the simulation period. Then, the Monte Carlo counter is incremented, and we repeat the whole process until 10^5 iterations are completed. Finally, the mean ($\bar{E}_{UE\_sim}$) and the 2.5th and 97.5th percentiles of the E_{UE_sim} distributionare are calculated across all simulation iterations to represent the emissions from UEs and their uncertainty.

S5. Simulating Emissions from UEs using probability of emission event occurrence

A significant limitation in estimating emissions from UEs through the simulation of POD and the identification of false negatives is the requirement for extensive temporal coverage of emissions measurements (i.e., either via continuous monitoring systems or frequent instantaneous screening surveys). However, not all sites are monitored sufficiently in the real world. To address this issue, we developed a second simulation approach that simulates UEs based on the probability of emission event occurrence rather than relying on the POD of deployed measurement technologies.

Prior to simulation, the following distributions are required to be created from the REs and PREs:

- The emission rate distribution (Q_{dist}) represents the expected emission rates for a given potential emission source category or equipment.
- The emission duration distribution (D_{dist}) represents the expected durations for a given potential emission source category or equipment.
- The probabilities represent the likelihood of an emission event occurrence ($P_{occurence}$) and not occurrence ($P_{not\_occurence}$) for a given potential emission source category or equipment based on D_{dist}.

Since multiple pieces of equipment can emit simultaneously and the emission of one piece is independent of another, sites with more equipment are more likely to have a higher probability of emissions occurring.

Noted, both equipment and bottom-up inventory are necessary to enhance the simulation results and prevent extrapolating emissions from incorrect source categories. For example, equipment or infrastructure on site can be used to determine the possible emission sources (e.g., emissions from flaring should not be extrapolated for a separator). Similarly, an accurate bottom-up inventory also can be used to constraint the simulation. For example, if liquid unloading never occurred. Then simulation should not extrapolate emissions from liquid unloading.
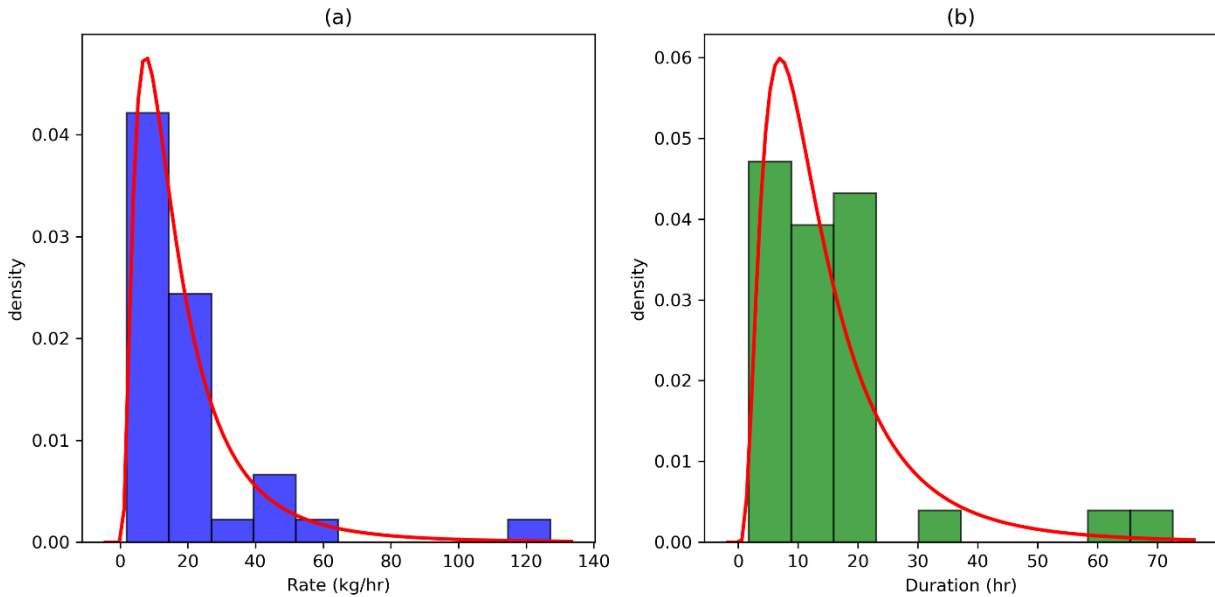
Figure S3. Example of using *Eq.13* to fit empirical rate (a) and duration (b) distributions

Since emission rates and durations tend to follow right-skewed distributions, we use a log-normal probability density functions to fit the empirical Q_{dist} and D_{dist} from REs and PREs (e.g., Figure S3).

$$P(v) = ae^{v^b} \hspace{6cm} Eq.13$$

Where v is the rate or duration sampled under the probability $P(v)$, and a and b are parameters required to fit the rate and duration for each source category or equipment type.

After fitting, the log-normal PDF with optimal a and b are used to create the expected rate and duration distributions, $Q_{\text{exp\_}dist}$ and $D_{\text{exp\_}dist}$, for UEs.

Unlike creating probability density functions, the combination of an emission event occurrence. Creating binomial distribution [11] based on two probabilities: $P_{occurence}$ and $P_{not\_occurence}$ can be described as follows:

$$B(x) = \binom{n}{x} P_{occurence}{}^{x} P_{not\_occurence}{}^{n-x} \qquad\qquad Eq.14$$

Where x is the proportion of time that a source can have an emission event in a given period (n). Since the probability is calculated using duration, $P_{occurence}$ and $P_{not\_occurence}$, it also describes how frequently a source can have an emission event.
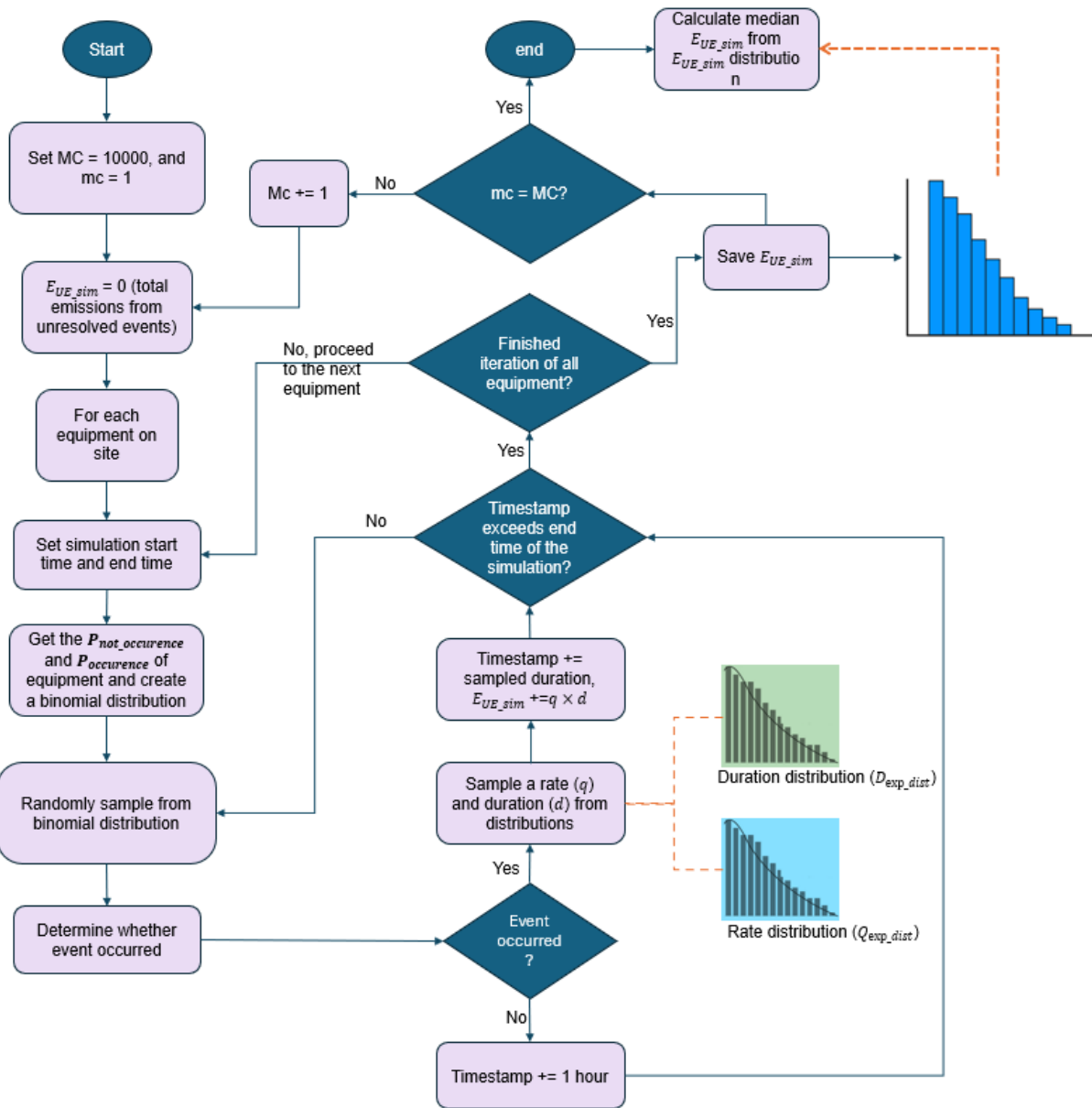
Figure S4. A workflow of simulating emissions from UEs by sampling events.

Figure S4 describes the workflow of simulations. The Monte Carlo simulation begins by setting the timestamp to the start time of the simulation and initializing emissions from UEs (E_{UE_sim}) to 0 kg. For each piece of equipment (source category), the simulation proceeds hourly, evaluating the likelihood of emission occurrence by sampling a binary outcome (0 or 1) based on the precalculated $P_{occurence}$ and $P_{not\_occurence}$ of that equipment. If an emission occurs, the emission rate (q) and duration (d) are sampled from the rate (Q_{exp_dist}) and duration (D_{exp_dist}) distributions, respectively, to define a UE. The E_{UE_sim} then updated by adding the emissions calculated from multiplying q and d, and the simulation time is incremented by d. If no emission event occurs, the

simulation time advances by one hour. This process is repeated until the end of the simulation time for each piece of equipment. The E_{UE_sim} is calculated by summing emissions from all sampled UEs across all equipment. The simulation is repeated for 10^5 iterations, and the median ($\bar{E}_{UE\_sim}$), along with the 2.5th and 97.5th percentiles of the E_{UE_sim} distribution, are calculated to represent the simulated emissions from UEs and their associated uncertainty.

S6. Synthetic emissions observations

Table S3. Synthetic CMS measurements in the case study No.1.

ID	site	equipment	start time	end time	rate (kg/hr)
CMS-89	A	Compressor-3	01-01-2024 2:16	01-01-2024 18:46	13.43743062
CMS-88	A	Compressor-2	01-01-2024 17:12	02-01-2024 0:32	11.0537834
CMS-87	A	Dehydrator-1	02-01-2024 8:38	03-01-2024 2:14	6.485984945
CMS-86	A	Dehydrator-1	03-01-2024 1:20	03-01-2024 17:55	9.745295575
CMS-85	A	Dehydrator-1	03-01-2024 23:33	04-01-2024 3:06	5.279977194
CMS-84	A	Dehydrator-1	04-01-2024 12:02	04-01-2024 20:25	44.44340994
CMS-83	A	Dehydrator-1	05-01-2024 12:21	05-01-2024 14:09	26.4754512
CMS-82	A	Dehydrator-1	05-01-2024 18:40	06-01-2024 15:03	10.2931667
CMS-81	A	Dehydrator-1	06-01-2024 12:55	07-01-2024 6:39	22.90488356
CMS-80	A	Dehydrator-1	07-01-2024 3:28	07-01-2024 7:34	4.38235222
CMS-79	A	Dehydrator-1	07-01-2024 15:50	08-01-2024 5:10	15.68792648
CMS-78	A	Dehydrator-1	08-01-2024 21:11	09-01-2024 5:36	23.01335768
CMS-77	A	Dehydrator-1	09-01-2024 4:54	09-01-2024 15:33	16.46214129
CMS-76	A	Dehydrator-1	09-01-2024 20:05	10-01-2024 10:21	6.575924082
CMS-75	A	Dehydrator-1	10-01-2024 9:17	11-01-2024 20:43	9.97428315
CMS-74	A	Dehydrator-1	12-01-2024 8:57	15-01-2024 9:31	39.60280338
CMS-73	A	Dehydrator-1	15-01-2024 9:19	15-01-2024 12:30	4.631917288
CMS-72	A	Compressor-2	15-01-2024 11:46	16-01-2024 6:06	127.1398731
CMS-71	A	Compressor-3	16-01-2024 11:53	17-01-2024 3:15	50.81348771
CMS-70	A	Compressor-2	17-01-2024 10:29	19-01-2024 23:15	9.865365612
CMS-69	A	Tank-2	20-01-2024 17:49	21-01-2024 0:07	7.830741333
CMS-68	A	Compressor-2	21-01-2024 7:16	22-01-2024 0:02	7.280364451
CMS-67	A	Compressor-3	22-01-2024 2:24	22-01-2024 7:15	1.872333732
CMS-66	A	Compressor-3	22-01-2024 6:48	23-01-2024 1:56	11.11957246
CMS-65	A	Tank-1	22-01-2024 13:05	23-01-2024 2:59	15.78909064
CMS-63	A	Dehydrator-1	23-01-2024 16:02	24-01-2024 8:27	19.49150927
CMS-64	A	Dehydrator-1	23-01-2024 16:02	24-01-2024 6:27	27.31177958
CMS-62	A	Dehydrator-1	24-01-2024 15:06	25-01-2024 1:46	17.92923359
CMS-61	A	Dehydrator-1	25-01-2024 16:45	26-01-2024 5:08	19.41097409
CMS-60	A	Dehydrator-1	26-01-2024 13:50	27-01-2024 6:36	22.35054016
CMS-59	A	Dehydrator-1	27-01-2024 1:45	27-01-2024 8:08	13.98306741
CMS-57	A	Dehydrator-1	27-01-2024 10:10	28-01-2024 3:15	13.09969511
CMS-58	A	Dehydrator-1	27-01-2024 10:10	27-01-2024 23:37	16.04159662

CMS-56	A	Dehydrator-1	28-01-2024 15:43	28-01-2024 23:59	10.05147194
CMS-55	A	Dehydrator-1	29-01-2024 15:48	30-01-2024 0:36	12.67874941
CMS-54	A	Dehydrator-1	31-01-2024 17:15	01-02-2024 3:30	60.47970498
CMS-53	A	Dehydrator-1	01-02-2024 13:45	01-02-2024 22:38	10.77638599
CMS-52	A	Dehydrator-1	02-02-2024 23:30	03-02-2024 6:10	24.7853662
CMS-51	A	Dehydrator-1	03-02-2024 11:03	03-02-2024 15:53	17.19845255
CMS-50	A	Dehydrator-1	04-02-2024 13:38	05-02-2024 8:05	23.45762222
CMS-49	A	Dehydrator-1	07-02-2024 4:05	07-02-2024 9:11	14.86192301
CMS-48	A	Dehydrator-1	07-02-2024 17:09	07-02-2024 21:40	13.72649872
CMS-47	A	Dehydrator-1	08-02-2024 8:39	08-02-2024 14:27	17.22924512
CMS-45	A	Dehydrator-1	08-02-2024 17:30	09-02-2024 4:10	11.86600299
CMS-46	A	Dehydrator-1	08-02-2024 17:30	09-02-2024 4:10	14.76924197
CMS-44	A	Dehydrator-1	10-02-2024 6:47	10-02-2024 16:31	6.821435342
CMS-43	A	Dehydrator-1	10-02-2024 14:50	10-02-2024 23:17	28.89126158
CMS-42	A	Dehydrator-1	11-02-2024 15:45	12-02-2024 5:38	123.3328614
CMS-41	A	Dehydrator-1	16-02-2024 11:51	16-02-2024 16:46	14.83360889
CMS-40	A	Dehydrator-1	22-02-2024 2:22	22-02-2024 9:08	17.60689626
CMS-39	A	Dehydrator-1	22-02-2024 11:25	23-02-2024 4:36	33.41612275
CMS-38	A	Compressor-2	23-02-2024 14:04	24-02-2024 3:23	18.51180616
CMS-37	A	Compressor-2	24-02-2024 8:34	24-02-2024 18:34	11.69312178
CMS-36	A	Compressor-2	27-02-2024 10:58	27-02-2024 15:44	14.44655555
CMS-35	A	Compressor-2	01-03-2024 17:52	01-03-2024 23:27	16.77220239
CMS-34	A	Compressor-2	03-03-2024 4:38	03-03-2024 22:15	17.15981442
CMS-33	A	Compressor-3	07-03-2024 5:57	07-03-2024 10:56	11.42898031
CMS-32	A	Compressor-2	07-03-2024 7:16	07-03-2024 15:02	16.23481555
CMS-31	A	Compressor-2	08-03-2024 12:23	10-03-2024 0:18	14.71608663
CMS-29	A	Compressor-3	14-03-2024 9:15	14-03-2024 23:52	15.29498708
CMS-30	A	Tank-1	14-03-2024 9:15	14-03-2024 23:52	14.74954203
CMS-28	A	Tank-1	15-03-2024 7:54	15-03-2024 19:43	10.83058592
CMS-27	A	Compressor-2	18-03-2024 15:35	19-03-2024 1:32	13.08735161
CMS-25	A	Separator-2	21-03-2024 16:45	22-03-2024 2:54	12.4923744
CMS-26	A	Dehydrator-2	21-03-2024 16:45	22-03-2024 2:54	15.49997366
CMS-24	A	Separator-2	22-03-2024 11:45	23-03-2024 4:40	19.45596602
CMS-23	A	Separator-2	23-03-2024 15:56	24-03-2024 8:16	20.77621499
CMS-22	A	Separator-2	29-03-2024 12:10	29-03-2024 18:10	50.5477992
CMS-21	A	Separator-2	05-04-2024 14:08	05-04-2024 17:58	19.2303107
CMS-20	A	Separator-2	05-04-2024 15:40	05-04-2024 20:41	53.27457756
CMS-19	A	Separator-2	06-04-2024 1:59	06-04-2024 5:50	18.95548269
CMS-18	A	Separator-2	09-04-2024 8:27	09-04-2024 19:36	18.53332709
CMS-17	A	Separator-2	10-04-2024 14:25	11-04-2024 0:11	140.6241274
CMS-16	A	Separator-2	11-04-2024 15:06	11-04-2024 22:43	55.89072104
CMS-15	A	Separator-2	12-04-2024 14:09	12-04-2024 22:15	29.79022037
CMS-14	A	Separator-1	13-04-2024 0:00	13-04-2024 8:05	14.72482916

CMS-13	A	Separator-1	14-04-2024 1:54	14-04-2024 5:54	16.01493411
CMS-11	A	Separator-1	16-04-2024 4:25	16-04-2024 10:40	13.04163146
CMS-12	A	Separator-1	16-04-2024 4:25	16-04-2024 10:40	9.677583744
CMS-10	A	Separator-1	17-04-2024 5:04	17-04-2024 14:09	24.53500301
CMS-9	A	Separator-1	18-04-2024 13:26	18-04-2024 20:51	14.93944563
CMS-8	A	Separator-1	18-04-2024 22:32	19-04-2024 2:41	17.65106764
CMS-7	A	Separator-1	19-04-2024 14:49	20-04-2024 2:49	35.81272269
CMS-6	A	Separator-2	20-04-2024 14:10	20-04-2024 16:35	77.00366334
CMS-5	A	Separator-1	22-04-2024 14:00	23-04-2024 10:07	77.63196097
CMS-4	A	Separator-1	26-04-2024 10:15	26-04-2024 16:38	10.80466042
CMS-3	A	Separator-1	27-04-2024 6:05	27-04-2024 13:57	16.03540446
CMS-2	A	Separator-1	28-04-2024 7:12	28-04-2024 19:16	11.16171355
CMS-1	A	Separator-1	29-04-2024 23:25	30-04-2024 4:48	29.86309642

Table S4. Synthetic flyover measurements in the case study No.1.

ID	site	equipment	detection time	detection	survey time	rate (kg/hr)
FLY-1	A			FALSE	07-01-2024 17:31	1538.3
FLY-2	A	Compressor-2	22-02-2024 19:40	TRUE	22-02-2024 15:40	53
FLY-3	A	Compressor-3	22-03-2024 19:40	TRUE	22-03-2024 16:40	64
FLY-4	A		05-04-2024 19:14	TRUE	05-04-2024 16:14	38.5

Table S5. Synthetic OGI measurements in the case study No.1.

ID	site	equipment	detection	survey time	number of leaks
OGI-1	A		FALSE	01-01-2024 17:31	0
OGI-2	A	Compressor-2	TRUE	01-02-2024 15:40	2
OGI-3	A	Separator-2	TRUE	01-03-2024 16:40	4
OGI-4	A		FALSE	01-04-2024 16:14	0

Table S6. Synthetic venting events in the case study No.1.

ID	site	equipment	start time	end time	total emissions (kg)
VFB-31	A	Compressor-3	01-01-2024 4:25	01-01-2024 4:35	182.796264
VFB-30	A	Tank-1	01-01-2024 13:34	01-01-2024 13:40	231.25869
VFB-29	A	Tank-1	02-01-2024 6:50	02-01-2024 6:57	159.2221714
VFB-28	A	Tank-1	03-01-2024 15:15	03-01-2024 15:20	263.071872
VFB-27	A	Compressor-2	05-01-2024 7:30	05-01-2024 7:35	339.0873
VFB-26	A	Tank-2	06-01-2024 0:40	06-01-2024 0:50	263.417292
VFB-25	A	Compressor-3	06-01-2024 11:30	06-01-2024 11:35	263.417292
VFB-24	A	Compressor-3	06-01-2024 17:25	06-01-2024 17:30	333.67572
VFB-23	A	Compressor-2	07-01-2024 1:30	07-01-2024 1:35	537.58866

VFB-22	A	Compressor-2	07-01-2024 9:30	07-01-2024 9:35	3515.56962
VFB-21	A	Compressor-2	07-01-2024 11:00	07-01-2024 11:05	335.886408
VFB-20	A	Compressor-3	08-01-2024 9:35	08-01-2024 9:40	311.91426
VFB-19	A	Compressor-2	10-01-2024 7:30	10-01-2024 7:35	390.3246
VFB-18	A	Compressor-2	10-01-2024 9:50	10-01-2024 9:55	401.447124
VFB-17	A	Tank-1	12-01-2024 9:45	12-01-2024 10:35	606.5022528
VFB-16	A	Compressor-3	23-01-2024 7:10	23-01-2024 7:15	416.323212
VFB-15	A	Tank-1	25-01-2024 9:00	25-01-2024 10:00	432.742176
VFB-14	A	Compressor-2	03-02-2024 7:40	03-02-2024 7:45	339.847224
VFB-13	A	Dehydrator-2	05-02-2024 14:14	16-02-2024 11:45	2.065004742
VFB-12	A	Compressor-2	10-02-2024 8:41	10-02-2024 8:45	307.9995
VFB-11	A	Compressor-3	10-02-2024 9:04	10-02-2024 9:07	480.05704
VFB-10	A	Compressor-2	10-02-2024 10:14	10-02-2024 10:16	541.158
VFB-9	A	Compressor-2	10-02-2024 11:00	10-02-2024 11:03	423.1395
VFB-8	A	Compressor-2	13-02-2024 8:30	13-02-2024 9:10	382.3367625
VFB-7	A	Compressor-1	25-02-2024 7:22	25-02-2024 7:24	413.12232
VFB-6	A	Compressor-1	26-02-2024 14:35	26-02-2024 14:37	615.999
VFB-5	A	Compressor-3	29-02-2024 17:20	29-02-2024 17:25	309.03576
VFB-4	A	Compressor-1	01-03-2024 11:45	01-03-2024 11:50	278.431548
VFB-3	A	Compressor-1	16-03-2024 11:10	16-03-2024 11:15	347.561604
VFB-2	A	Compressor-2	18-03-2024 9:10	18-03-2024 9:15	212.77872
VFB-1	A	Compressor-1	20-03-2024 14:45	20-03-2024 14:47	513.98496
VFB-49	A	Compressor-3	02-04-2024 10:23	02-04-2024 10:26	454.11216
VFB-48	A	Compressor-1	06-04-2024 9:20	06-04-2024 9:26	245.70876
VFB-47	A	Compressor-3	20-04-2024 13:19	20-04-2024 13:24	288.0502435
VFB-46	A	Compressor-3	22-04-2024 3:03	22-04-2024 3:14	123.0951273
VFB-45	A	Compressor-3	22-04-2024 6:40	22-04-2024 6:45	320.918208
VFB-44	A	Compressor-1	23-04-2024 8:20	23-04-2024 8:25	415.77054
VFB-43	A	Compressor-3	23-04-2024 11:40	23-04-2024 11:45	385.903224
VFB-42	A	Compressor-2	26-04-2024 0:12	26-04-2024 0:35	53.88552
VFB-41	A	Compressor-1	26-04-2024 22:20	26-04-2024 22:30	119.377152
VFB-40	A	Compressor-2	27-04-2024 8:24	27-04-2024 8:35	147.8502273
VFB-39	A	Tank-3	27-04-2024 15:08	27-04-2024 15:24	122.4585863
VFB-38	A	Compressor-1	29-04-2024 23:13	29-04-2024 23:20	176.3286857
VFB-37	A	Compressor-2	29-04-2024 23:20	29-04-2024 23:26	229.5124
VFB-36	A	Compressor-3	30-04-2024 2:05	30-04-2024 2:13	266.693025
VFB-35	A	Compressor-2	30-04-2024 4:10	30-04-2024 4:19	221.6445
VFB-34	A	Tank-2	30-04-2024 6:37	30-04-2024 6:50	1152.179409
VFB-33	A	Compressor-2	30-04-2024 8:12	30-04-2024 8:23	109.6970182
VFB-32	A	Compressor-3	30-04-2024 9:50	30-04-2024 9:58	182.61204

Table S7. Synthetic CMS measurement in the case study No.2.

ID	site	equipment	start time	end time	rate (kg/hr)
CMS-1	B	Compressor-3	01-01-2024 2:16	01-01-2024 18:46	13.43743062
CMS-2	B	Compressor-2	01-01-2024 17:12	02-01-2024 0:32	11.0537834
CMS-3	B	Tank-1	02-01-2024 8:38	03-01-2024 2:14	6.485984945
CMS-4	B	Dehydrator-1	03-01-2024 1:20	03-01-2024 17:55	9.745295575
CMS-5	B	Tank-1	03-01-2024 23:33	04-01-2024 3:06	5.279977194
CMS-6	B	Separator-1	04-01-2024 12:02	04-01-2024 20:25	44.44340994
CMS-7	B	Dehydrator-1	05-01-2024 12:21	05-01-2024 14:09	26.4754512
CMS-8	B	Separator-2	05-01-2024 18:40	06-01-2024 15:03	10.2931667
CMS-9	B	Dehydrator-1	06-01-2024 12:55	07-01-2024 6:39	22.90488356
CMS-10	B	Separator-3	07-01-2024 3:28	07-01-2024 7:34	4.38235222
CMS-11	B	Tank-1	07-01-2024 15:50	08-01-2024 5:10	15.68792648
CMS-12	B	Dehydrator-1	08-01-2024 21:11	09-01-2024 5:36	23.01335768
CMS-13	B	Dehydrator-1	09-01-2024 4:54	09-01-2024 15:33	16.46214129
CMS-14	B	Dehydrator-1	09-01-2024 20:05	10-01-2024 10:21	6.575924082
CMS-15	B	Dehydrator-1	10-01-2024 9:17	11-01-2024 20:43	9.97428315
CMS-16	B	Tank-1	12-01-2024 8:57	15-01-2024 9:31	39.60280338
CMS-17	B	Dehydrator-1	15-01-2024 9:19	15-01-2024 12:30	4.631917288
CMS-18	B	Compressor-2	15-01-2024 11:46	16-01-2024 6:06	127.1398731
CMS-19	B	Compressor-3	16-01-2024 11:53	17-01-2024 3:15	50.81348771
CMS-20	B	Compressor-2	17-01-2024 10:29	19-01-2024 23:15	9.865365612
CMS-21	B	Tank-2	20-01-2024 17:49	21-01-2024 0:07	7.830741333
CMS-22	B	Compressor-2	21-01-2024 7:16	22-01-2024 0:02	7.280364451
CMS-23	B	Compressor-3	22-01-2024 2:24	22-01-2024 7:15	1.872333732
CMS-24	B	Wellhead	22-01-2024 6:48	23-01-2024 1:56	11.11957246
CMS-25	B	Tank-1	22-01-2024 13:05	23-01-2024 2:59	15.78909064
CMS-26	B	Dehydrator-1	23-01-2024 16:02	24-01-2024 8:27	19.49150927
CMS-27	B	Compressor-1	23-01-2024 16:02	24-01-2024 6:27	27.31177958
CMS-28	B	Dehydrator-1	24-01-2024 15:06	25-01-2024 1:46	17.92923359
CMS-29	B	Separator-2	25-01-2024 16:45	26-01-2024 5:08	19.41097409
CMS-30	B	Dehydrator-1	26-01-2024 13:50	27-01-2024 6:36	22.35054016
CMS-31	B	Dehydrator-1	27-01-2024 1:45	27-01-2024 8:08	13.98306741
CMS-32	B	Separator-2	27-01-2024 10:10	28-01-2024 3:15	13.09969511
CMS-33	B	Compressor-1	27-01-2024 10:10	27-01-2024 23:37	16.04159662
CMS-34	B	Separator-2	28-01-2024 15:43	28-01-2024 23:59	10.05147194
CMS-35	B	Dehydrator-1	29-01-2024 15:48	30-01-2024 0:36	12.67874941
CMS-36	B	Tank-2	31-01-2024 17:15	01-02-2024 3:30	60.47970498

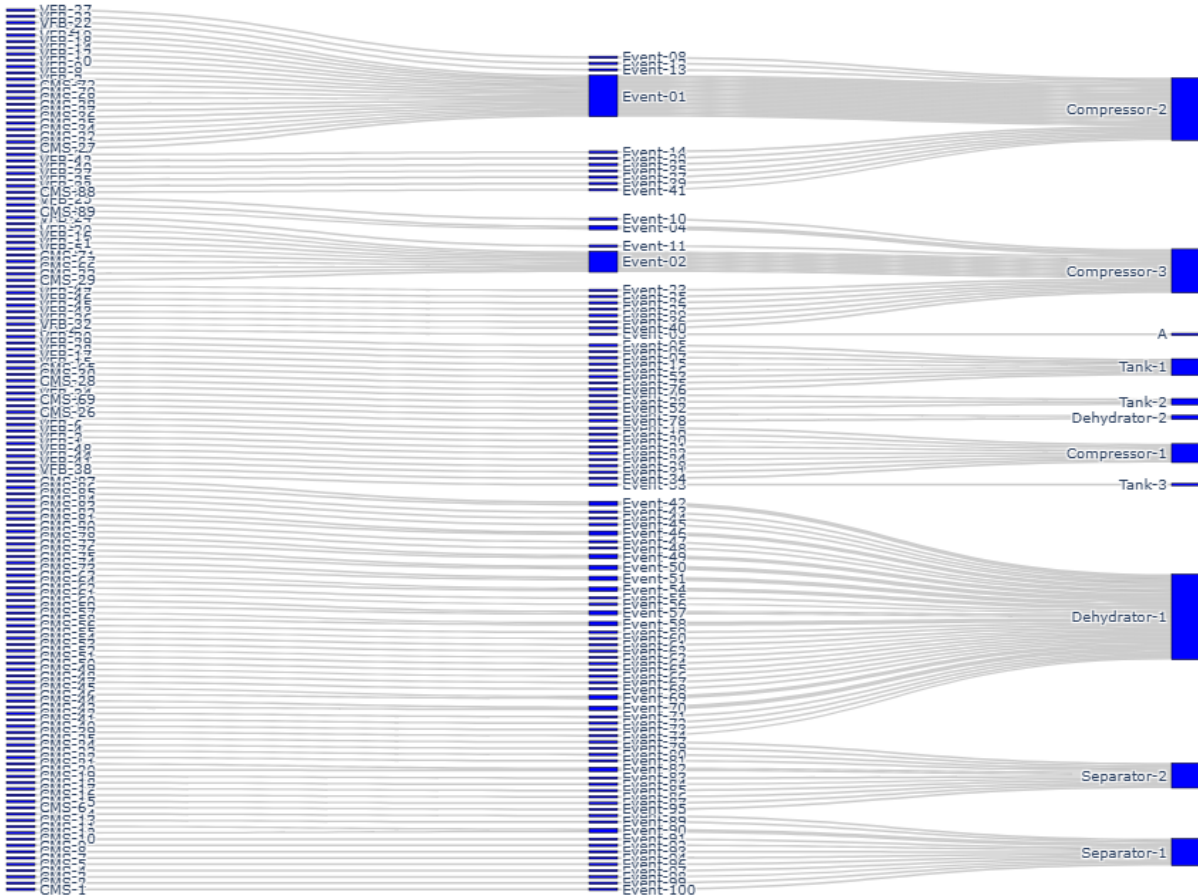## S7. Parameters and assumptions used in case studies

Figure S5. Sankey diagram describing how emission observations are merged to emission events and how emission events are attributed to equipment in the fictitious site.

For case study No.1, we initiated 92 PREs and 49 REs. By applying Allen's interval algebra and source attribution results, we merged 41 events, reducing the total number of events to 100, consisting of 61 PREs and 39 REs. Figure S5 illustrates the process of merging emission observations to create events and their allocation to each fictitious piece of equipment.

We assume a quantification uncertainty of +/-60% across all events to demonstrate the proposed equations. After merging the events, only one PRE requires duration to be estimated using our proposed duration simulation. Following parameters and assumptions are used to simulate the duration of this PRE: a default LPR of 0.006 leaks/day/site, a 7-day visitation interval, one leak per site at initialization, 10 global leaks, one active leak, and an operator bonus of 0.5. For the remaining PREs, durations were determined based on measured start and end times from CMS observations. Following the findings from Daniels et al. [3], the associated duration uncertainties were assumed to range from 0 to twice the measured durations.

The simulation of emissions below the MDL was applied to estimate total emissions from UEs. The following parameters, datasets, and assumptions were used: five CMS sensors were installed

on-site; wind speed data from Permian Basin was downloaded from ERA5 [12]; three flight passes were conducted; the component-scale emission rate was sampled from the empirical component measurements [8]; and the POD equations from InsightM aircraft and Qube sensors (MIQ, 2024) were used to simulate emissions from UEs [9,13].

References

1. Allen, J. F. Maintaining Knowledge about Temporal Intervals. *Commun. ACM* **1983**, *26* (11), 832–843. https://doi.org/10.1145/182.358434.
2. Sherwin, E. D.; Chen, Y.; Ravikumar, A. P.; Brandt, A. R. Single-Blind Test of Airplane-Based Hyperspectral Methane Detection via Controlled Releases. *Elementa* **2021**, *9* (1). https://doi.org/10.1525/elementa.2021.00063.
3. Daniels, W. S.; Jia, M.; Hammerling, D. M. Estimating Methane Emission Durations Using Continuous Monitoring Systems. *Environ. Sci. Technol. Lett.* **2024**, *11* (11), 1187–1192. https://doi.org/10.1021/acs.estlett.4c00687.
4. Intergovernmental Panel on Climate Change. *2006 IPCC Guidelines for National Greenhouse Gas Inventories: Volume 1. General Guidance and Reporting*; National Greenhouse Gas Inventories Programme: Hayama, Japan, 2006.
5. Ku, H. H. Notes on the Use of Propagation of Error Formulas. *J. Res. Natl. Bur. Stand., Sect. C* **1966**, *70C* (4), 263. https://doi.org/10.6028/jres.070c.025.
6. Fox, T. A.; Gao, M.; Barchyn, T. E.; Jamin, Y. L.; Hugenholtz, C. H. An Agent-Based Model for Estimating Emissions Reduction Equivalence among Leak Detection and Repair Programs. *J. Clean. Prod.* **2021**, *282*, 125237. https://doi.org/10.1016/j.jclepro.2020.125237.
7. Koehler, E.; Brown, E.; Haneuse, S. J.-P. A. On the Assessment of Monte Carlo Error in Simulation-Based Statistical Analyses. *Am. Stat.* **2009**, *63* (2), 155–162. https://doi.org/10.1198/tast.2009.0030.
8. Rutherford, J. S.; Sherwin, E. D.; Ravikumar, A. P.; Heath, G. A.; Englander, J.; Cooley, D.; Lyon, D.; Omara, M.; Langfitt, Q.; Brandt, A. R. Closing the Methane Gap in U.S. Oil and Natural Gas Production Emissions Inventories. *Nat. Commun.* **2021**, *12*. https://doi.org/10.1038/s41467-021-25017-4.
9. Conrad, B. M.; Tyner, D. R.; Johnson, M. R. Robust Probabilities of Detection and Quantification Uncertainty for Aerial Methane Detection: Examples for Three Airborne Technologies. *Remote Sens. Environ.* **2023**, *288*, 113499. https://doi.org/10.1016/j.rse.2023.113499.
10. Bell, C. S.; Ilonze, C.; Duggan, A.; Zimmerle, D. Performance of Continuous Emission Monitoring Solutions under a Single-Blind Controlled Testing Protocol. *Environ. Sci. Technol.* **2023**, *57* (14). https://doi.org/10.1021/acs.est.2c09235.
11. Jowett, G. H. The Relationship between the Binomial and F Distributions. *Statistician* **1963**, *13* (1), 55. https://doi.org/10.2307/2986663.
12. Hersbach, H.; Bell, B.; Berrisford, P.; Biavati, G.; Horányi, A.; Muñoz Sabater, J.; Nicolas, J.; Peubey, C.; Radu, R.; Rozum, I.; Schepers, D.; Simmons, A.; Soci, C.; Dee, D.; Thépaut, J.-N. ERA5 Hourly Data on Single Levels from 1940 to Present. *Copernicus Climate Change Service (C3S) Climate Data Store (CDS)* **2023**. https://doi.org/10.24381/cds.adbb2d47.

13. MiQ. *Monitoring Technology Compatibility Assessment Qube Axon*; MiQ, 2024. Retrieved from https://miq.org/document/qube-compatibility-assessment-2.